

Heat Transfer in a Radiatively Heated Particle-laden Laminar Jet Flow

K.C.Y. Kueh^{1,3}, T.C.W. Lau^{1,3}, Z. Alwahabi^{2,3} and G.J. Nathan^{1,3}

¹School of Mechanical Engineering
University of Adelaide, South Australia 5005, Australia

²School of Chemical Engineering
University of Adelaide, Adelaide, South Australia 5005, Australia

³Centre for Energy Technology
University of Adelaide, Adelaide, South Australia 5005, Australia

Abstract

An investigation on the heat transfer within a radiatively heated laminar particle-laden flow was performed using the spatially and temporally-resolved laser-induced phosphorescence (LIP) technique. It was found that particle concentration is higher near the edge of the jet ($r/D \approx 0.5$) as compared to the jet axis. This non-uniform particle concentration distribution was found to have a direct impact on particle temperatures, T_p , likely due to the effects of inter-particle re-radiation. Additionally, it was found that the radiative heating of the particles induces complex phenomenon such as buoyancy, re-radiation, and clustering, even for this simple laminar flow field. These results are internally consistent and extremely repeatable, justifying the need for further investigation.

Introduction

Heat transfer within particle-laden jet flows is poorly-understood, field that has been the subject of many investigations due to complexity of simultaneously-occurring mechanisms such as fluid-particle interactions, inter-particle collisions, buoyancy, scattering and shadowing within the flow [9-11]. This lack of detailed understanding limits the ability to improve current process efficiencies involving particle-laden flows and hinders development of new technologies. As an example, particle receivers have been identified as having strong potential among emerging concentrated solar thermal (CST) technologies to achieve much higher temperatures than the commercially available 580°C due to their lower overall costs and highly efficient heat transfer from direct concentrated solar irradiation [7]. However, one limitation on the rate of development is sub-optimal heat transfer within the receiver. Hence, it is important to have a more comprehensive understanding of fundamental processes that occur within these systems, including the effect of flow dynamics on heat transfer.

Previously, investigations of the heat transfer within particle-laden flows has been performed mostly on pre-heated jets [5,8,12-13]. In each of the cases reported, a hot “core” was observed, in which tracer particles in the centre of the jet flow were hotter than those on the outside. However, little is known about the heat transfer process of radiatively-heated particles downstream from the pipe exit. This is relevant for the understanding in non-isothermal systems such as the heating of falling particles through an aperture in solar particle receivers.

The present investigation utilises a well-characterised radiative heat source in the form of the Solid-state Solar Thermal Simulator (SSSTS), capable of delivering a flux of up to 36.6MW/m² [1]. The SSSTS operates at a peak wavelength of 910nm wavelength, which is absorbed by particles but not by air.

The radiative heat absorption of single stationary and spherical particles has been extensively modelled and measured for a range of particle sizes, ranging from $d_p = 2\mu\text{m}$ to 800 μm [4,6-7,15,17-18]. These measurements have consistently shown that particle temperature is heavily dependent on the heating intensity, particle absorptivity, particle diameter, and ambient gas thermal conductivity [14]. However, the significance of these parameters on particle temperatures within a turbulent flow of multiple, interacting particles has not been experimentally investigated in flows with poly-dispersed particles. This is because in-situ, non-intrusive temperature measurement of micron-sized particles within a flow is challenging. Most previous thermometry methods measured gas temperature using thermocouples, with the solid particles within the flow either assumed to be small enough to be modelled as gas, or the temperature inferred from fundamental heat transfer equations [2-3]. These methods are highly idealised and do not represent realistic heat transfer within a particle-laden flow field. Additionally, large errors (>50K) in thermocouple measurements of particle temperatures have been reported [8]. In contrast, the laser-induced phosphorescence (LIP) technique enables spatially and temporally-resolved particle measurements to be collected [9].

This paper aims to provide new insight into the heat transfer within a particle-laden laminar jet flow under well-characterised heating with high flux radiation downstream of the pipe exit through first-of-a-kind spatially and temporally resolved measurements.

Experimental Arrangement

The particles were made from ZnO:Zn thermophosphors (TPs), which were introduced from a fluidised-bed feeder through a 500mm long, 12.8mm diameter round pipe ($L/d = 39.66$) into a 300mm \times 300mm wind tunnel, as shown in Figure 1. This TP was selected due to its high phosphorescent emission and sensitivity to temperatures $\leq 625^\circ\text{C}$. The pipe was placed in the centre of a small wind tunnel to generate nominally uniform co-flow with negligible boundary effects within the imaging section. Air flow in the fluidised bed feeder was controlled with a mass flow controller (Alicat Scientific, MC 20 SLPM) to maintain a volumetric flow rate of 13 L/min (equivalent to 1.7 m/s at the pipe exit). The ZnO:Zn particles were between 100 μm and 250 μm in diameter.

An Nd:YAG laser beam operated at 6.24 ± 0.41 mJ was used to excite ZnO:Zn particles seeded within the flow at pipe exit. The excitation laser was manipulated by a three-lens system to form a 0.3mm \times 18 mm laser sheet at the test section. Phosphorescent emission from the thermophosphors were then recorded with an ICCD camera (PI-Max/PI-Max2, Princeton Instruments) through a 40mm spacer and an f/2.8 Tamron lens. A beam splitter was used to divide the imaging region into two

equal 18.2mm (H) \times 9.6mm (W) images, starting at the pipe exit. This minimizes time-delay and angular distortion errors typical of using traditional two-camera systems. The camera gain, gate width and gate delay were set to 5, 26ns and 51ns respectively, to maximize the phosphorescence signal collection. To heat the particles, the Solid-state Solar Thermal Simulator (SSSTS) which consists of multi fibre-coupled laser diode modules, each producing 80W of power was used. A unique feature of the SSSTS is that the output is collimated by an adjustable three-lens system, which allows for controllable output with a maximum flux of 36.6MW/m^2 [1]. The heating beam has a diameter of 10.5mm , spanned $0.2 \leq x/D \leq 0.8$ and was placed 2mm below the pipe exit. Its beam path was located such that it was offset by 7° from that of the excitation laser. A water-cooled power meter (Gentec model HP100A-4KW- HE) acted as the SSSTS beam dump, while also providing in-situ laser power measurements at a sample frequency of 10 Hz. Thirteen different heat fluxes between 2.1MW/m^2 and 35.3MW/m^2 were investigated. And for each case, 2000 single-shot images were collected with the first 100 shots taken with the SSSTS turned off.

To relate phosphorescent emissions to temperature, a calibration experiment was performed with the same experimental setup described, with the exception that a TP-coated plate in a temperature-controlled oven is located in place of the wind tunnel. A detailed description of the experimental setup is presented by Kueh [9].

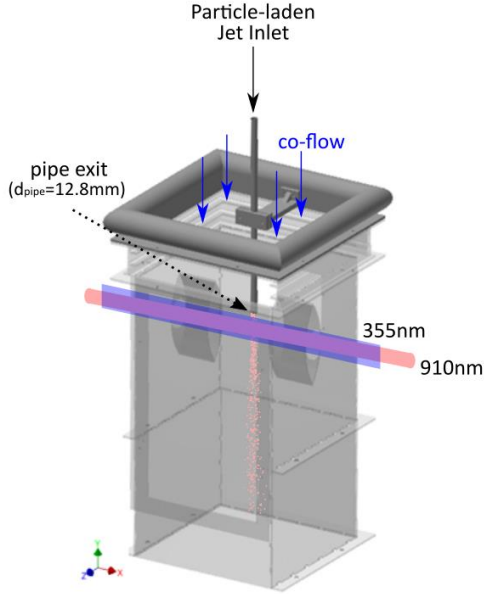


Figure 1: Wind tunnel system used in experiment. A 12.8mm diameter pipe was used to seed ZnO:Zn particles (red dots exiting pipe) into the system. The blue laser path indicates the 355nm Nd:YAG laser, while the red indicates that of the 910nm SSSTS heating beam.

A simple first-order heat transfer model of a single moving particle subjected to radiative heating at high fluxes was used to estimate particle temperature changes, ΔT_p within a system similar to that of the experimental setup. This was used to perform a sensitivity study of the effects of slip velocity, particle diameter, particle mass loading on ΔT_p . The heat transfer modes taken into account were: (1) radiative heating of the particle, $Q_{heat} = \alpha \Phi A_p F_{12}$, (2) convective cooling between the particle and surrounding flow, $Q_{conv} =$

$h A_{p,s} (T_p - T_a)$, (3) re-radiation, $Q_{rad,cool} = \sigma A_{p,s} (T_p^4 - T_a^4) F_{23}$ and (4) heat gain within the particle, $Q_{gain} = \dot{m}_p c_p \frac{\Delta T_p}{dt}$. These heat transfer modes may be expressed with the following energy balance equation (1):

$$\alpha \Phi A_p F_{12} = h A_{p,s} (T_p - T_a) + \varepsilon \sigma A_{p,s} (T_p^4 - T_a^4) F_{23} + \dot{m}_p c_p \frac{\Delta T_p}{dt} \quad (1)$$

where $\alpha = 0.15$ is the absorptivity [14], Φ is the laser flux, $A_p = \pi r_p^2$ is the particle cross-sectional area, r_p is the particle radius, $F_{12} = 0.5$ is the view factor of heat flux on particles, $\varepsilon = 0.69$ is the emissivity, $\sigma = 5.67 \times 10^{-8} \text{ W/m}^2\text{K}^4$ is the Stefan-Boltzmann constant, $A_{p,s}$ is the particle surface area, $h = \frac{Nu}{d_p} / k_g$ is the convective heat transfer coefficient, $Nu = 2 + (0.4 \times Re^{0.5} + 0.06 \times Re^{\frac{2}{3}}) \times Pr^{0.4} \left(\frac{\mu_a}{\mu}\right)^{0.4}$ is the Nusselt number, $Re = \frac{\rho V_{slip} d_p}{\mu}$ is the Reynolds number, V_{slip} is the slip velocity, k_p is the thermal conductivity of the particle, k_g is the thermal conductivity of the gas, \dot{m}_p is the particle mass flow rate, T_{film} is the film temperature, t is the particle residence time, T_p is the particle temperature, T_a is the atmospheric temperature, and F_{23} is the view factor between particles. The specific heat of the particles was modelled following earlier work [19] as:

$$c_p = 53.999 + 7.851 \times 10^{-4} T_{film} - 5.868 \times 10^{-5} T_{film}^2 - 127.5 T_{film}^{-0.5} + 1.9376 \times 10^{-6} T_{film}^2 \quad (2)$$

Results

Figure 2 presents the contour map of particle temperature (top row) and number density (bottom row) of at radiative heating fluxes, Φ , of (a) 6.1MW/m^2 , (b) 20.6MW/m^2 , (c) 35.3MW/m^2 . The red dotted line indicates the start and end of the heating region ($0.2 < x/D < 0.8$) with the beam paths entering from the left. It can be seen that particle concentration is highest at the edge of the jet flow ($r/D \rightarrow 0.5$) as compared to the centre ($r/D \rightarrow 0$) for all 3 flux cases. This is consistent with previous studies [10-11] where it was found that for particle Stokes numbers, $Sk \lesssim 1$, turbophoresis, a phenomenon that causes particles to migrate towards regions with low turbulent intensities, is dominant. This is the same range as the Stokes number for the present ZnO:Zn particles, defined as $Sk = \frac{\rho_p d_p v_r}{18 \mu_g}$, which is $Sk \approx 1.42$.

Additionally, it can be seen from the temperature maps in Figure 2 that T_p in the heating region ($0.2 < x/D < 0.8$) tends to be higher at $r/D \rightarrow 0.5$. This is attributed to the greater particle residence times in this region, as the particle velocity, which can be estimated from a laminar velocity profile, is lower in this region. Since particle residence times strongly affects T_p , as shown in equation (1), T_p at $r/D \rightarrow 0$ is expectedly lower than those at $r/D \rightarrow 0.5$. Also, it should be noted that in this region ($0.2 < x/D < 0.8$), high T_p regions also coincides with regions of high particle concentration, which may also indicate significant heat transfer by inter-particle re-radiation heat transfer in this region, and/or lower convective losses.

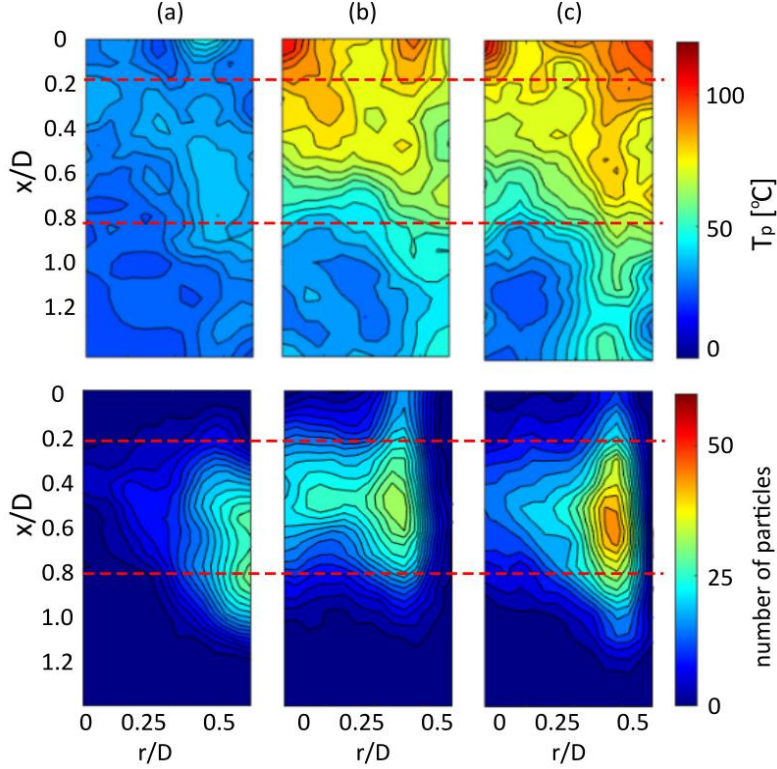


Figure 2: Contour plots of mean particle temperatures (top) and number density (bottom) calculated over 2000 instantaneous images for heat fluxes at (a) 6.1 MW/m², (b) 20.6 MW/m², (c) 35.3 MW/m².

A perhaps surprising finding in the present investigation is that the highest mean temperatures were recorded upstream from the heating region ($x/D < 0.2$), even though this would be impossible with the cold-flow aerodynamics, which only convects particles downstream from the exit plane. In particular, the regions of highest particle temperature upstream from the radiating heating region are found near to both the jet axis ($r/D \rightarrow 0$) and the jet edge ($r/D \rightarrow 0.5$), of the jet flow upstream of the direct heating region. Given that the same particle temperature measurement technique was applied to room temperature cases where the SSSTS was not turned on and the T_p measured was between 22°C and 27°C, this finding was determined to be an actual occurrence, and not a bias in the measurement.

Figure 3 presents a scatter plot of the distributions of T_p at $0.7 < \frac{x}{D} < 0.8$, for the cases with radiant fluxes of: (a) 6.1 MW/m², (b) 20.6 MW/m², (c) 35.3 MW/m². Also shown is the line best fit (plotted in red). The mean particle temperature profile here is as follows:

$$T_p(r) = a * \left(1 - \frac{r^2}{R^2}\right) + b \quad (4)$$

where a and b are constants that depend on the fluxes. An example of these values are presented in Table 1. Here, b values increase with respect to heat flux. It can be seen that the mean particle

temperature profile correlates strongly to the inverse of the particle velocity profile.

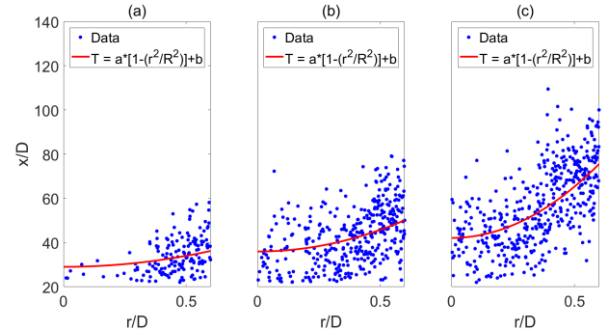


Figure 3: Influence of r/D location on particle temperature, T_p , at $0.7 \leq x/D \leq 0.8$ for flux: (a) 6.1 MW/m², (b) 20.6 MW/m², (c) 35.3 MW/m². Red lines are the modelled velocity profiles.

| Flux [MW/m ²] | a | b |
|---------------------------|-------|-------|
| 6.1 | -12.8 | 41.2 |
| 20.6 | -25.1 | 61.1 |
| 35.3 | -59.4 | 101.5 |

Table 1: a and b constants for various heat fluxes to model mean particle temperature with equation (4).

Discussion

An explanation for the high T_p found at $x/D < 0.2$ is the heat transfer from the heated particles in the heating region ($0.2 < x/D < 0.8$) to the particles upstream of them ($x/D < 0.2$). Since radiation occurs at the speed of light [12], the governing factor for such heat transfer mechanism would be the view factor, indicated as F_{23} in equation (1). It follows that regions with higher particle number density ($r/D \rightarrow 0.5$) would experience

higher re-radiation and absorption rates, where secondary heating from re-radiation of nearby particles would increase overall particle temperature.

Another possibility for the higher T_p in this region is buoyancy. As particles are heated, air in the boundary layer of the particles is also heated, resulting in a fluid region around the particle having a lower density than the bulk flow. This density difference may be sufficiently high to induce buoyancy effects near and around the particles. However, given the maximum particle temperature, $T_{p,max}$, measured in the present investigation is $\sim 250^\circ\text{C}$, and the large fluid velocities relative to the expected buoyancy-induced velocities, buoyancy is only expected to be significant in regions of low fluid velocity, i.e., at $r/D \rightarrow 0.5$.

Additional and direct evidence for likely role of buoyancy in convecting hot particles upstream can be found in the observation that particles were observed to have deposited on outside of the pipe upstream from the heating region, after, and only after, radiative heating with high fluxes ($\phi > 12.2 \text{ MW/m}^2$). In addition, flow visualisation of the co-flow reconfirmed that no flow recirculation is present in the co-flow around the jet under isothermal conditions. It is plausible that these hot particles could be entrained into the jet and/or transfer heat through the walls of the pipe. It is further plausible that these hot particles could transfer heat to the core of the jet by radiation, hence the reason why the particles in the jet axis exit the pipe hot, although further research is required to confirm or otherwise these potential explanations.

Conclusions

Temperatures of particles ($100\mu\text{m} \leq d_p \leq 250\mu\text{m}$) in a radiatively-heated, laminar particle-laden jet flow was measured using spatially and temporally-resolved laser-induced phosphorescence (LIP). Number density was also found by particle counting from the images. It was found that particle concentration was higher in the outside of the jet ($r/D \rightarrow 0.5$) as compared to the centre, in line with turbophoresis effects seen in previous investigations. This distribution has a direct impact in particle temperatures, T_p , likely due to the effects of inter-particle re-radiation. Additionally, the radiative heating under these conditions generates complex phenomenon that cause hot particles to be found upstream of the heated zone. The most likely cause for this observation is the role of buoyancy, combined with 3-dimensional re-radiation, although further work is required to confirm these plausible explanations.

Additional support for the deduce role of buoyancy is the observation that particles attach to the outside of the pipe when, and only when, the fluxes are sufficiently high. These phenomenon warrant further investigation.

Acknowledgments

We gratefully acknowledge support from the Australian Research Council through its Discovery grant 150102230 and Linkage Grant LE130100127. The financial support from the Institute of Mineral and Energy Resource (IMER) and the Faculty of Engineering, Computer & Mathematical Science (ECMS) at The University of Adelaide is acknowledged.

References

- [1] Alwahabi, Z., Kueh, K.C.Y., Nathan G.J., Cannon, S., A Novel Radiation Source Supplying 30,000 suns by Fibre Optical Probe: Demonstration of Particles Heating by Radiation, *Optics Express*, **24**, 2016, 1444-1453.
- [2] Anoop, K.B., Sundararajan, T., Das, S.K., Effect of Particle Size on the Convective Heat Transfer in Nanofluid in the

- Developing Region, *International J. Heat and Mass Transfer*, **52**, 2009, 2189-2195.
- [3] Collier, A.P., Hayhurst, A.N., Richardson, J.L., Scott, S.A., The Heat Transfer Coefficient between a Particle and a Bed (Packed or Fluidised) of Much Larger Particles, *Chemical Engineering Science*, **59**, 2004, 4613-4620.
- [4] Fincke, J.R., Jeffery, C.L., Spjut, R.E., Measurement of the Emissivity of Small Particles at Elevated Temperatures, *Optical Engineering*, **27**, 1988, 684-690.
- [5] Fond, B., Abram, C., Heyes, A.L., Kempf, A.M., Beyrau, F., Simultaneous Temperature, Mixture Fraction and Velocity Imaging in Turbulent Flows using Thermographic Phosphor Tracer Particles, *Optics Express*, **20**, 2012, 22118-22133.
- [6] Foss, W.R., James Davis, E., Transient Laser Heating of Single Solid Microspheres, *Chemical Engineering Communications*, **152-153**, 1996, 113-138.
- [7] Grena R., Thermal Simulation of a Single Particle in a Falling-particle Solar Receiver, *Solar Energy*, **83**, 2009, 1186-1199.
- [8] Jovicic, G., Zigan, L., Will, S., Leipertz, A., Phosphor Thermometry in Turbulent Hot Gas Flows Applying Dy:YAG and Dy:Er:YAG Particles, *Measurement Science and Technology*, **26**, 2015.
- [9] Kueh, K.C.Y., Lau, T.C.W., Nathan, G.J., Alwahabi, Z., Single-shot Planar Temperature Imaging of Radiatively Heated Fluidized Particles, *Optics Express*, **25**, no.23, 2017, 28764-28775.
- [10] Lau, T.C.W., Nathan, G.J., Influence of Stokes Number on the Velocity and Concentration Distributions in Particle-laden Jets, *J. Fluid Mech.*, **757**, 2014, 432-457.
- [11] Lau, T.C.W., Nathan, G.J., The Effects of Stokes Number on Particle Velocity and Concentration Distributions in a Well-characterised, Turbulent, Co-flowing Two-phase Jet, *J. Fluid Mech.*, **809**, 2016, 72-110.
- [12] Lavieille, P., Delconte, A., Blondel, D., Lebouche, M., Lemoine, F., Non-intrusive Temperature Measurements using Three-color Laser-induced Fluorescence, *Experiments in Fluids*, **37**, 2004, 706-716.
- [13] Lavieille, P., Lemoine, F., Lavergne, G., Lebouche, M., Evaporating and Combusting Droplet Temperature Measurements using Two-color Laser-induced Fluorescence, *Experiments in Fluids*, **31**, 2001, 45-55.
- [14] Monazam, E.R., Maloney, D.J., Lawson, L.O., Measurements of heat capacities, temperatures, and absorptivities of single particles in an electrodynamic balance, *Review of Scientific Instruments*, **60**, 1989, 3460-3465.
- [15] Pesic, R., Radoicic, T.K., Boskovic-Vragolovic, N., Arsenijevic, Z., Grbavcic, Z., Heat transfer between a packed bed and a larger immersed spherical particle, *International Journal of Heat and Mass Transfer*, **78**, 2014, 130-136.
- [16] Schunk, L.O., Solar thermal dissociation of Zinc Oxide Reaction Kinetics, Reactor Design, Experimentation, and Modeling (Doctoral dissertation), ETH Zürich, 2008.
- [17] Spjut, R.E., Sarofim, A.F., Longwell, J.P., Laser heating and particle temperature measurement in an electrodynamic balance, *Langmuir*, **1**, 1985, 355-360.
- [18] Tripathi, A., Vaughn, C.L., Maswadeh, W., Meuzelaar, H.L.C., Measurement and modeling of individual carbonaceous particle temperature profiles during fast CO2 laser heating: Part 2. Coals, *Thermochemica Acta*, **388**, 2002, 199-213.
- [19] Zinc oxide (ZnO) Debye temperature, heat capacity, density, melting point, vapor pressure, hardness, *Springer Berlin Heidelberg*, 1999.
- [20] Holman, J.P., Heat Transfer: Tenth Edition, *McGraw Hill Higher Education*, 2010.